Supplement of Atmos. Chem. Phys., 15, 13569–13584, 2015
http://www.atmos-chem-phys.net/15/13569/2015/
doi:10.5194/acp-15-13569-2015-supplement

Atmospheric Chemistry and Physics
Open Access

Supplement of

Reactive uptake of ammonia to secondary organic aerosols: kinetics of organonitrogen formation

Y. Liu et al.

Correspondence to: J. Liggio (john.liggio@ec.gc.ca)

Supporting Information

OH concentration estimation method.

The OH concentration during the photochemical oxidation of m-xylene were calculated based upon the decay of m-xylene and the known second-order rate constant with respect to OH (Atkinson and Arey, 2003), while it was calculated based upon the difference between the measured decay of α-pinene and the predicted decay curve due to consumption by O_3 in ozonolysis of α-pinene experiments. During the ozonolysis of α-pinene, OH can be formed through decomposition of peroxides in the dark (Zhang and Zhang, 2005). Both O_3 and OH react with α-pinene. Thus,

$$-\frac{dc_{\mathrm{pin\_O_3}}}{dt} = k_{2,\mathrm{pin-O_3}} c_{\mathrm{O_3}} c_{\mathrm{pin}} \qquad \text{(S1)}$$

$$-\frac{dc_{\mathrm{pin\_OH}}}{dt} = k_{2,\mathrm{pin-OH}} c_{\mathrm{OH}} c_{\mathrm{pin}} \qquad \text{(S2)}$$

where $c_{\mathrm{pin\_O_3}}$, $c_{\mathrm{pin\_OH}}$ and c_{pin} are the concentration α-pinene consumed by O_3, OH and the measured concentration of α-pinene (molecules cm^{-3}), respectively; $c_{\mathrm{O_3}}$ and c_{OH} are the concentration of O_3 and OH (molecules cm^{-3}); $k_{2,\mathrm{pin-O_3}}$ and $k_{2,\mathrm{pin-OH}}$ are the second-order rate constant for O_3 and OH with respect to α-pinene (cm^3 molecule^{-1} s^{-1}), respectively. Using the measured concentration of O_3 and α-pinene, we can predict the concentration of α-pinene consumed by O_3. Namely,

$$\Delta c_{\mathrm{pin}_{\mathrm{O_3},t_i}} = k_{2,\mathrm{pin-O_3}} c_{\mathrm{O_3},t_i} c_{\mathrm{pin},t_i} \Delta t \qquad \text{(S3)}$$

where, t_i is the time.

If we assume that alpha-pinene decreases only due to reaction with O_3 or OH, then

$$c_{\mathrm{pin}_{\mathrm{OH},t_i}} = c_{\mathrm{pin},t_i} - c_{\mathrm{pin\_O}_{3},t_i} \qquad \text{(S4)}$$

The results using this estimation method are shown in Figure S1 .

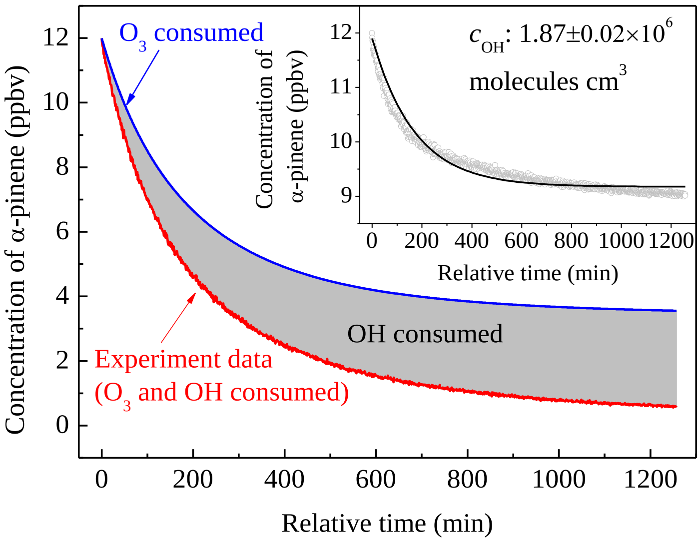

Figure S1. Demonstration of the OH concentration calculation in an ozonolysis of α-pinene experiment (Exp. P8). The inset graph shows the curve fitting with exponential decay of α-pinene consumed by OH.

Details of the uptake model.

The aerosol radius can be written in terms of m_{NOC}

$$a = \left(\frac{3m_{\mathrm{NOC}}}{4\pi\rho} + a_0^3\right)^{\frac{1}{3}} \qquad \text{(S5)}$$

where a_0 and ρ represent the initial seed particle radius and the density of the organic mass. Equation (S6) can then be derived by substituting Eq. (1) with Eq. (S5),

$$\int_{m_0}^{m} (bm_{\mathrm{NOC}} + d)^{-2/3}\,\mathrm{d}m_{\mathrm{NOC}} = \int_{t_0}^{t} \gamma_{\mathrm{obs}}\, \pi c_{\mathrm{NH}_3} < c > F_{\mathrm{h}} \mathrm{d}t \qquad \text{(S6)}$$

Where, $b = \frac{3}{4\pi\rho}$, $d = a_0^3$. The initial seed particle radii were measured in each experiment and the density of the organic mass was assumed to be 1.4 g cm^{-3}

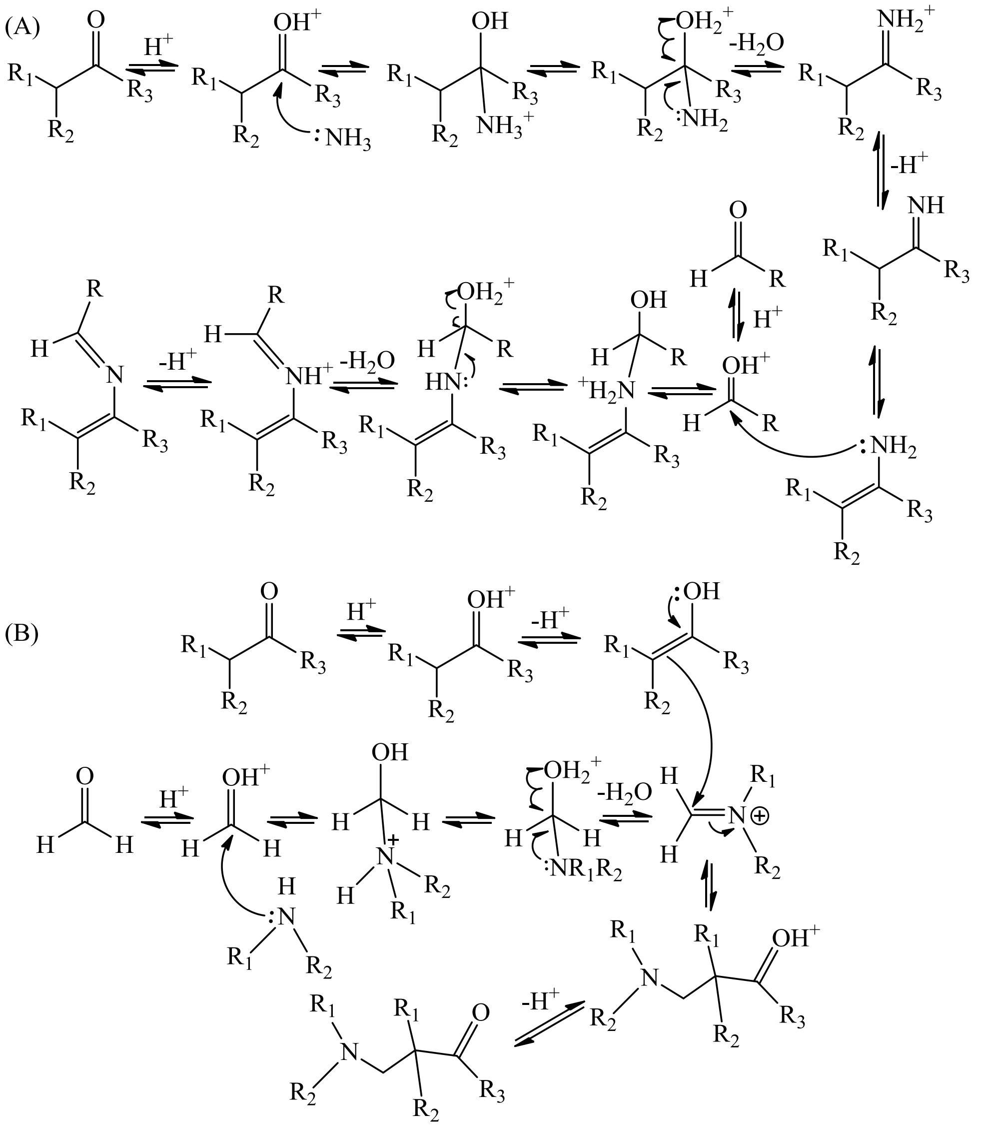

Scheme S1. Generic (A) reaction mechanism to form Schiff-base and (B) Mannich reaction mechanism for reactions between carbonyl compounds and ammonia/ammonium.

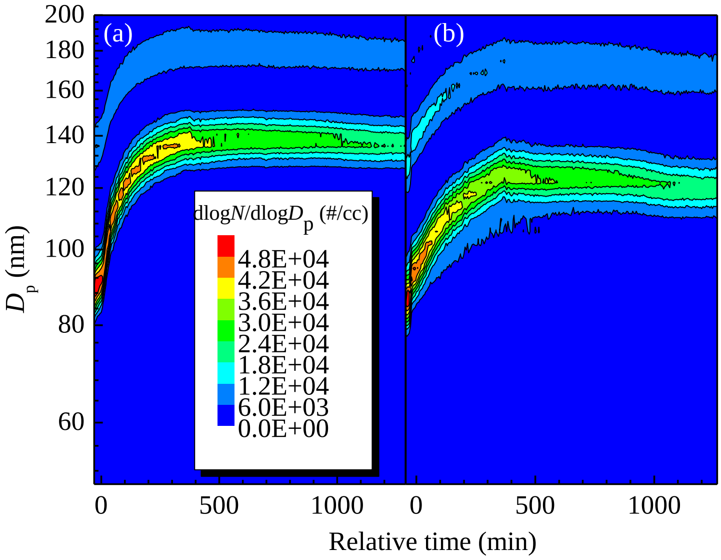

Figure S2. Changes of particle size as a function of time during (a) the ozonolysis of α–pinene (Exp. P6) and (b) UV-H_2O_2 oxidation of m-xylene (Exp. M16).

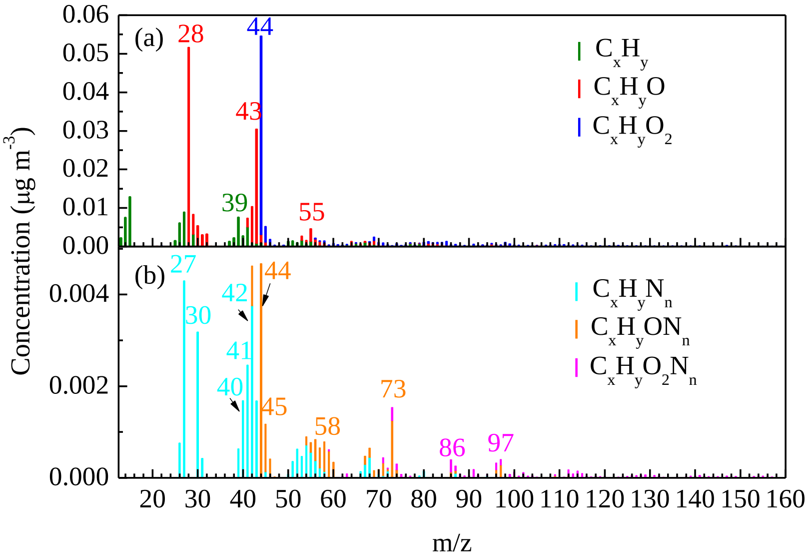

Figure S3. Mass spectra of (a) non-N-containing species fragments and (b) N-containing species fragments in the SOA formed by OH oxidation of m-xylene in the presence of 66 ppbv NH_3 (Exp. M16).

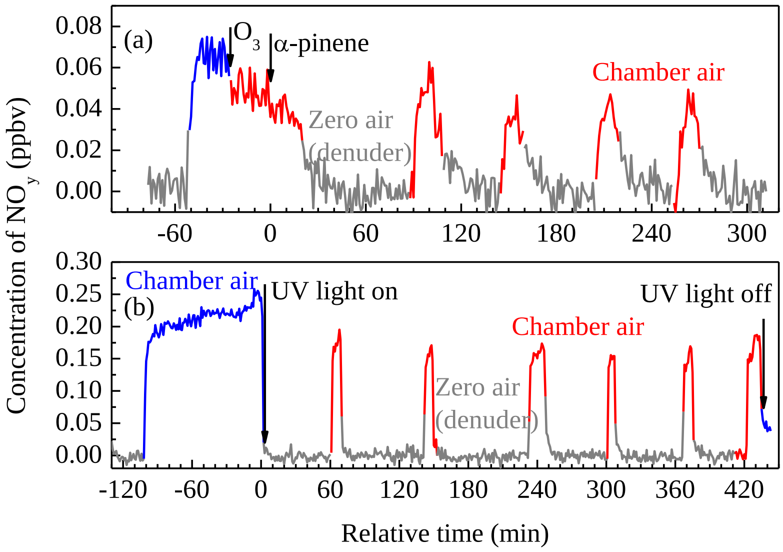

Figure S4. Gaseous NO_y concentration in the chamber for (a) O_3 oxidation of α–pinene (Exp. P13) and (b) OH oxidation of m-xylene (Exp. M20).

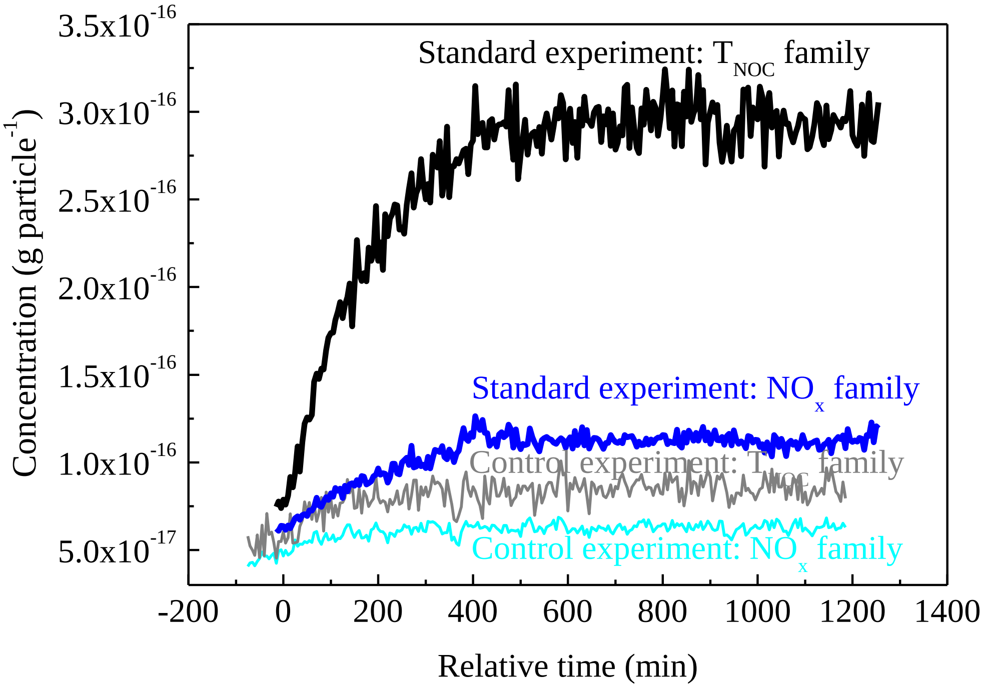

Figure S5. Comparison of the NOx fragment family and T_{NOC} (total nitrogen) concentrations in typical (Exp. P8) and control experiments (Exp. B7). The experimental conditions in the control experiment are the same as that in standard experiment with the exception of 0 ppbv of α–pinene.

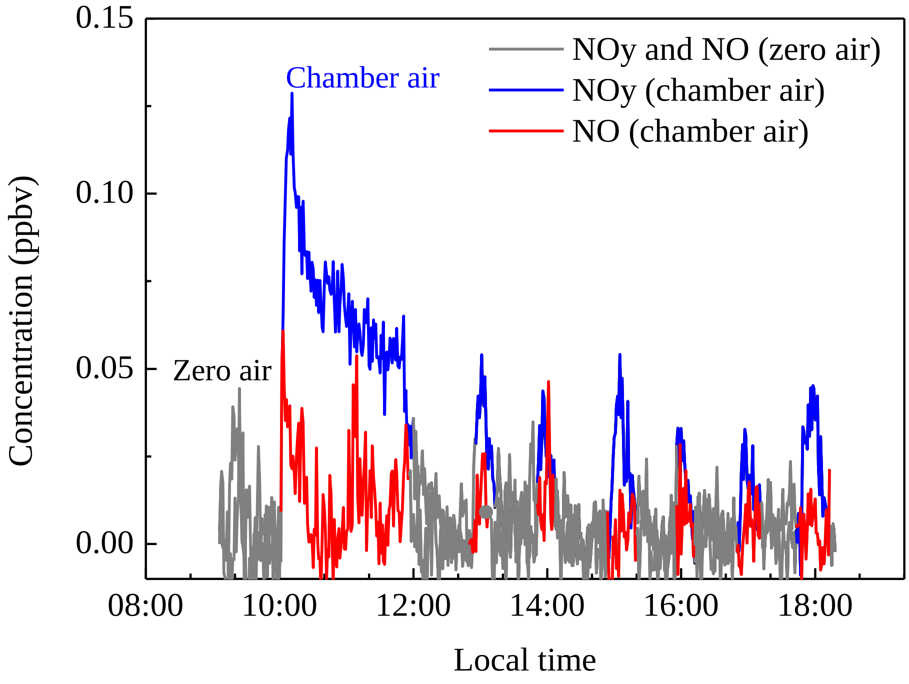

Figure S6. Typical concentration of NO in the chamber (Exp. P14).

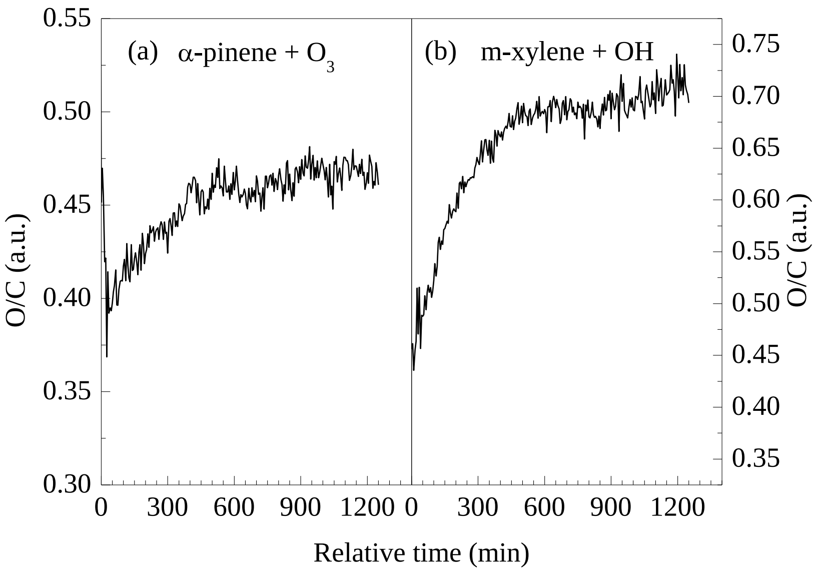

Figure S7. Typical O/C evolution for (A) ozonolysis of α-pinene (Exp. P13) and (B) OH oxidation of m-xylene (Exp. M15).

Table S1. Assignment of IR bands.

Wavenumber of observed IR bands (cm^{-1})	Assignment	Ranges reported in literatures (cm^{-1})
3490	NH_2 asymmetric stretching (Simons, 1978)	~3500
3240	NH_3^+ asymmetric stretching (Simons, 1978) Secondary amide N-H stretching (Stuart, July 2004)	3200-2800 3300-3250
3060	Ar-H Stretching (Simons, 1978) Secondary amide amide II overtone	3100-3000 3100-2060
2962	CH_3 symmetric stretching (Simons, 1978;Stuart, July 2004)	2972-2952
2860	CH_3 asymmetric stretching or CH_2 stretching (Simons, 1978;Stuart, July 2004)	2882-2862 or 863-2843
2675, 2630	Combination bands of $-NH_3^+$ and $-NH_2^+$ deformation vibration or $-NH^+$ stretching (Simons, 1978)	2800-2400 (1°) 2700-2300 (2°) 2700-2330 (3°)
2195	C≡N stretching in C=C-C≡N (Simons, 1978) N=C=N stretching (Simons, 1978)	2195 2170-2100
1725	C=O stretching (Schwartz et al., 2010;Stuart, July 2004)	1725-1700
1660	C=N stretching (Nguyen et al., 2013;Lin-Vien et al., 1991;Bruns et al., 2010) Oxime C=N-OH stretching (Stuart, July 2004) Nitrite N=O stretching (Stuart, July 2004)	1650-1590 1690-1620 1680-1650
1640	NH_2 bending (Simons, 1978;Stuart, July 2004) C=N stretching (Bruns et al., 2010) NO_2 asymmetric stretching in $RONO_2$ (Bruns et al., 2010;Stuart, July 2004)	1627-1590;1638-1602 1690-1620 1660-1620
1563	NH_2 bending (Nguyen et al., 2013) Secondary amide N-H bending, C-N stretching (Stuart, July 2004) C=C stretching (Stuart, July 2004)	1563 1560-1530 1600-1430
1423	C-H bending (Bruns et al., 2010) C-O-H bending (in-plane) C-N stretching (Lin-Vien et al., 1991)	1485-1430 1430 1430-1390
1315	C-N stretching (Simons, 1978;Stuart, July 2004) NO_2 symmetric stretching in $RONO_2$ (Bruns et al., 2010)	1360-1250 1280
1120	SO symmetric stretching in Na_2SO_4 (Stuart, July 2004;Miller and Wilkins, 1952)	1120
1050	C-O-C stretching (Simons, 1978) C-N-C asymmetric stretching (Lin-Vien et al., 1991)	1050-1010 1058
950	O-H deformation vibration (Simons, 1978)	950-900 965-930

	Oxime N-O stretching (Stuart, July 2004)	
870	NH_2 wag(out-of-plane) (Simons, 1978) C-H bending (out-of-plane) (Stuart, July 2004) NO symmetric stretching in $RONO_2$ (Bruns et al., 2010)	900-650 900-690 860
785	NH_2 wag(out-of-plane) (Simons, 1978) C-N-C symmetric stretching (Lin-Vien et al., 1991) C-H bending (out-of-plane) (Stuart, July 2004)	900-650 762 900-690
740	NH_2 wag(out-of-plane) (Simons, 1978) C-H bending (out-of-plane) (Stuart, July 2004)	900-650 900-690

Table S2. Reactive uptake coefficients to form NOC and NH_4^+

Exp No[a].	($\gamma_{t,ini}$)[b]	(γ_{NH4})[c]	($\gamma_{t,final}$)[d]
P1	$\mathbf{7.15\pm0.30\times10^{-3}}$	$\mathbf{6.20\pm0.28\times10^{-3}}$	$\mathbf{4.87\pm0.27\times10^{-5}}$
P2	$\mathbf{9.87\pm0.33\times10^{-3}}$	$\mathbf{8.96\pm0.31\times10^{-3}}$	$\mathbf{4.04\pm0.25\times10^{-5}}$
P3	$\mathbf{2.02\pm0.10\times10^{-2}}$	$\mathbf{1.78\pm0.09\times10^{-2}}$	$\mathbf{1.74\pm0.31\times10^{-5}}$
4P	$\mathbf{1.36\pm0.05\times10^{-2}}$	$\mathbf{1.14\pm0.04\times10^{-2}}$	$\mathbf{2.16\pm0.40\times10^{-5}}$
P5	$\mathbf{5.57\pm0.09\times10^{-3}}$	$\mathbf{4.45\pm0.06\times10^{-3}}$	$\mathbf{5.20\pm0.16\times10^{-5}}$
P6	$\mathbf{1.15\pm0.04\times10^{-2}}$	$\mathbf{1.01\pm0.04\times10^{-2}}$	$\mathbf{2.06\pm0.32\times10^{-5}}$
B7	**-**	**-**	**-**
P8	$\mathbf{1.12\pm0.07\times10^{-2}}$	$\mathbf{9.61\pm0.62\times10^{-3}}$	$\mathbf{6.10\pm0.47\times10^{-5}}$
P9	$\mathbf{9.05\pm1.14\times10^{-3}}$	$\mathbf{7.94\pm1.09\times10^{-3}}$	$\mathbf{0\pm0.46\times10^{-5}}$
P10	$\mathbf{9.11\pm0.46\times10^{-3}}$	$\mathbf{8.41\pm0.45\times10^{-3}}$	**-**
P11	$\mathbf{7.41\pm0.48\times10^{-3}}$	$\mathbf{6.82\pm0.45\times10^{-3}}$	$\mathbf{6.09\pm0.33\times10^{-5}}$
P12	$\mathbf{6.55\pm0.40\times10^{-3}}$	$\mathbf{6.00\pm0.37\times10^{-3}}$	$\mathbf{4.62\pm0.29\times10^{-5}}$
P13	$\mathbf{7.03\pm0.40\times10^{-3}}$	$\mathbf{6.57\pm0.39\times10^{-3}}$	**-**
P14	$\mathbf{7.39\pm0.37\times10^{-3}}$	$\mathbf{6.69\pm0.36\times10^{-3}}$	**-**
M15	$\mathbf{1.03\pm0.05\times10^{-2}}$	$\mathbf{3.40\pm0.46\times10^{-3}}$	$\mathbf{0\pm2.53\times10^{-5}}$
M16	$\mathbf{5.92\pm0.31\times10^{-3}}$	$\mathbf{2.30\pm0.23\times10^{-3}}$	$\mathbf{0\pm2.12\times10^{-5}}$
M17	$\mathbf{5.43\pm0.22\times10^{-3}}$	$\mathbf{1.98\pm0.22\times10^{-3}}$	**-**
M18	$\mathbf{3.29\pm0.17\times10^{-3}}$	$\mathbf{6.62\pm0.14\times10^{-4}}$	$\mathbf{0\pm3.00\times10^{-5}}$
M19	$\mathbf{3.44\pm0.19\times10^{-3}}$	$\mathbf{9.15\pm0.14\times10^{-4}}$	$\mathbf{0\pm2.64\times10^{-5}}$
M20	$\mathbf{3.67\pm0.13\times10^{-3}}$	$\mathbf{5.37\pm0.08\times10^{-4}}$	**-**

[a]. P, B and M represent α–pinene, blank and m-xylene experiments, respectively. [b]. Uptake coefficient leading to NOC including NH_x fragments in the derivation from 0 to 150 min. [c]. Uptake coefficient for NH_3 leading to inorganic ammonium (ie: using NH_x fragments only). [d]. Uptake coefficient leading to NOC including NH_x fragments in the derivation from 400 to 1200 min.

References:

Atkinson, R., and Arey, J.: Atmospheric Degradation of Volatile Organic Compounds, Chem. Rev., 103, 4605-4638, doi: 10.1021/cr0206420, 2003.

Bruns, E. A., Perraud, V., Zelenyuk, A., Ezell, M. J., Johnson, S. N., Yu, Y., Imre, D., Finlayson-Pitts, B. J., and Alexander, M. L.: Comparison of FTIR and Particle Mass Spectrometry for the Measurement of Particulate Organic Nitrates, Environ. Sci. Technol., 44, 1056-1061, doi: 10.1021/es9029864, 2010.

Lin-Vien, D., Colthup, N. B., Fateley, W. G., and Grasselli, J. G.: The Handbook of Infrared and Raman Characteristic Frequencies of Organic Molecules, A Division ofHarcourt Brace & Company 525 B Street, Suite 1900, San Diego, California 92101-4495, 1991.

Miller, F. A., and Wilkins, C. H.: Infrared Spectra and Characteristic Frequencies of Inorganic Ions, Anal. Chem., 24, 1253-1294, doi: 10.1021/ac60068a007, 1952.

Nguyen, T. B., Laskin, A., Laskin, J., and Nizkorodov, S. A.: Brown carbon formation from ketoaldehydes of biogenic monoterpenes, Faraday Discuss., 165, 473-494, doi: 10.1039/C3FD00036B, 2013.

Schwartz, R. E., Russell, L. M., Sjostedt, S. J., Vlasenko, A., Slowik, J. G., Abbatt, J. P. D., Macdonald, A. M., Li, S. M., Liggio, J., Toom-Sauntry, D., and Leaitch, W. R.: Biogenic oxidized organic functional groups in aerosol particles from a mountain forest site and their similarities to laboratory chamber products, Atmos. Chem. Phys., 10, 5075-5088, doi: 10.5194/acp-10-5075-2010, 2010.

Simons, W. W.: The Sadtler Handbook of Infrared Spectra. , William Walter Simons, Philadelphia: Sadtler Research Laboratories, 1978.

Stuart, B. H.: Infrared Spectroscopy: Faundamentals and Applications, Wiley, 244 pp., July 2004.

Zhang, D., and Zhang, R.: Ozonolysis of a-pinene and b-pinene: Kinetics and mechanism, J. Chem. Phys., 122, 114308-114318, doi: 10.1063/1.1862616g, 2005.